Anodic etching of SiC in alkaline solutions

D H van Dorp[1], J L Weyher[2] and J J Kelly[1]

[1] Condensed Matter and Interfaces, Debye Institute, Utrecht University, Princetonplein 1,
3508 TA Utrecht, The Netherlands
[2] Applied Materials Science, Institute for Molecules and Materials, Radboud University
Nijmegen, Toernooiveld 1, 6526 ED Nijmegen, The Netherlands

E-mail: D.H.vanDorp@phys.uu.nl, J.J.Kelly@phys.uu.nl and J.Weyher@science.ru.nl

Abstract
The photoelectrochemistry of silicon carbide in alkaline solution was
investigated with a view to wet-chemical etching applications. Anodic
dissolution and passivation of the p-type semiconductor was observed in the
dark; illumination with supra-bandgap light was required for oxidation of
the n-type electrode. At low KOH concentrations and low light intensities,
diffusion-controlled etching is observed for n-type SiC. We show that
open-circuit photoetching can be used for defect revealing. Furthermore,
based on the electrochemical properties of silicon carbide and silicon, we
expect various material-selective etching processes to be possible.

1. Introduction

There is strong renewed interest in silicon carbide (SiC) for
device applications. With a favourable lattice constant and
coefficient of thermal expansion, it can serve as substrate for
epitaxial growth of group III-nitrides [1]. In many application
areas, for instance those related to aerospace, automotive and
petroleum industries, there is a need for electronic devices
that can operate at high power levels, high temperatures, high
frequencies and in harsh environments. Silicon (Si) cannot
meet these requirements; SiC can [2–4]. In addition, because
of its exemplary chemical and mechanical properties SiC, in
combination with Si, is finding wider application in sensors
and micro-electromechanical systems (MEMS) [5–9].

Because of its extreme chemical stability, there are no
(simple) wet-chemical etchants for SiC available. As a result,
physical (dry) etching dominates in SiC device technology.
Reactive-ion etching (RIE) and related methods are widely
used [10]. These techniques generally involve complex and
expensive equipment. In addition, RIE can give rise to
damaged surfaces with surface and bulk electronic states,
which may be detrimental to the performance of electronic
devices. The chemical stability of SiC is related to its
strong covalent bonds resulting from a wide bandgap and a
valence-band edge at low energy. As a result there are no
stable oxidizing agents capable of removing valence electrons
for surface bonds, i.e. from the valence band; consequently
electroless etching is not possible. Chemical etching is
only possible under rather extreme conditions, e.g. in molten
sodium hydroxide/potassium hydroxide (NaOH/KOH)

eutectic [11]. This approach can reveal crystallographic
defects but is not suitable for device fabrication.

Anodic or electrochemical etching offers an alternative
to open-circuit etching. By using a voltage source and a
counter electrode, one can regulate the electric field in the
space-charge layer of the semiconductor and thus the valence-
band hole concentration at the interface with the solution. The
localization of holes in surface bonds leads to bond rupture
and dissolution of the semiconductor. This can obviously
occur with a p-type semiconductor in the dark, while an n-
type semiconductor must be illuminated to generate minority
carriers.

SiC has been previously used as electrode in
electrochemical studies [12–14]. Photoanodic etching of n-
type SiC in acidic fluoride solution has been investigated by
Shor and co-workers. They showed that, depending on the
experimental conditions, one can either obtain mesoporous
or uniform etching [15, 16]. The latter can be exploited
for patterning of devices. Okijie *et al* have used selective
photoanodic etching of SiC p–n junctions in HF solution to
produce membranes for MEMS applications [8]. For anodic
etching, it is essential to avoid the formation of a passivating
surface oxide, SiO_2, which can be formed on SiC and is soluble
in aqueous HF solution. It is known that SiO_2 is also soluble in
alkaline solution; many aspects of Si MEMS technology make
use of this property. Surprisingly, there has been little attention
paid to electrochemical etching of SiC at high pH. In this paper
we show that such an approach can be used both for uniform
etching and passivation of SiC. Photoanodic etching of n-type
SiC with a counter electrode but without a voltage was also

used. We consider the results in relation to two possible uses of the approach: defect revealing and layer-selective etching.

2. Experimental details

Single-crystal 6H-SiC (n-type) and 4H-SiC wafers (n- and p-type) (0 0 0 1) were obtained from Cree (United States) and Umicore (Belgium). The n-type wafers were oriented on-axis, nitrogen-doped and had a resistivity varying between 0.01 and 0.07 Ω cm. The p-type wafer (Cree) was oriented 8° off-axis, aluminium doped and had a resistivity of 3.86 Ω cm. All samples used in this study had a Si polar face. For the electrochemical experiments, a circular opening was defined on the samples using a Si_3N_4 mask. The diameter of the opening was 2 mm. Ohmic contacts to the p-type SiC were made by evaporating a 300 nm thick layer of Al/Ta/Au on the back side of the wafer. The metallized wafer was subsequently annealed at 850 °C for 10 min. The n-type wafers were contacted using a 300 nm Ti/Au layer followed by a 1 s annealing step at 1000 °C. The samples were mounted as a rotating disc electrode (RDE). Electrochemical measurements were performed in a three-electrode cell with a platinum counter electrode and a saturated calomel electrode (SCE) as a reference. For open circuit photoetching experiments, Ohmic contacts were made by evaporating a Ti layer, 100 nm thick, without any additional heat treatment.

During electrochemical experiments, the rotation rate was fixed at 50 rpm. All potentials are given with respect to SCE. A potentiostat (EG&G Princeton Applied Research, PAR-273-A) computer-controlled by LabVIEW was used to measure the current–potential curves in the dark and under illumination. The curves were recorded at a constant scan rate of 5 mV s^{-1} towards positive potential. The light source used for the electrochemical experiments was a 500 W Hg arc-lamp with a power supply (Oriel 66941). UV light from the beam was directed on the sample using a dichroic mirror (280–400 nm). In order to increase the light intensity a plano convex lens was used to focus the beam on the electrode. The light intensity was varied with neutral density (ND) filters. Before the measurement, the samples were rinsed with acetone.

For the open-circuit photoetching experiments, a 450 W Xe lamp was used with a power supply (Oriel 66924). The SiC electrode was directly connected to a platinum counter electrode without an additional voltage source. The potential of the SiC is, in this case, determined by the kinetics of the reactions occurring at both the semiconductor and the counter electrode. For open-circuit photoetching to be possible in KOH solution, the onset of the oxygen reduction reaction at platinum must be at a potential more positive than the onset of the photoanodic oxidation of SiC [17].

Chemical etching was performed in a KOH/NaOH eutectic with 10% MgO (E+M etch) at temperatures in the range of 520–540 °C for 5–10 min [11]. All chemicals used were p.a. quality and obtained from Merck.

The etch rate was determined by measuring the etch depth with a surface profiler (Alpha-Step 500) and the surface morphology after etching was examined using a differential interference contrast (DIC) optical microscope (Nicon ECLYPSE ME 600), an atomic force microscope (Digital Instruments Nanoscope IIIa) and a scanning electron microscope (SEM Jeol 6330).
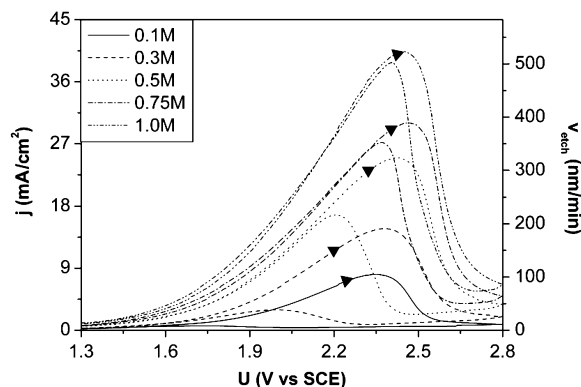

Figure 1. Current-potential curves for p-type 4H-SiC at different KOH concentrations at 20.5 °C. The right axis shows the calculated etch rate (see the text).

3. Results and discussion

3.1. Electrochemistry of p-type SiC

Figure 1 shows current density–potential (j–U) plots for a p-type 4H-SiC electrode at different KOH concentrations at 20.5 °C. For all curves, a typical active/passive transition is observed. At lower potentials the current increases with increasing potential. This is related to the exponential dependence of the hole concentration at the surface on the band bending in the space-charge layer. The holes driven to the surface oxidize the semiconductor and a soluble silicate product and CO are formed [13]:

$$SiC + 8OH^- + 6h^+(VB) \rightarrow [Si(OH)_2O_2]^{2-} + CO + 3H_2O. \tag{1}$$
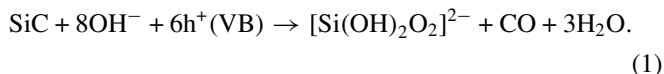
In previous work we showed that the holes are used exclusively for the oxidation of the semiconductor; no oxygen is formed [13]. Six holes are required to dissolve one formula unit of SiC. This allows us to convert current density to etch rate (see the right axis, figure 1 and subsequent figures). Above a critical current density (j_p) the electrode passivates, as sparingly soluble SiO_2 is formed:

$$SiC + 6OH^- + 6h^+ \rightarrow SiO_2 + CO + 3H_2O. \tag{2}$$
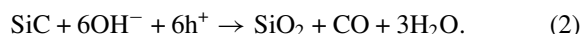
Under steady-state conditions, the rate of oxide formation in the passive range is equal to the rate of chemical dissolution of the oxide. The current in the return scan from positive to negative potential is much lower than in the forward scan due to the oxide on the surface. When the surface oxide starts to be removed, the current recovers somewhat. After complete removal of the oxide, the current recovers fully. As expected, the recovery time decreases with increasing KOH concentration: from 4 min in a 0.1M KOH solution down to 1.5 min in 1.0M KOH solution. The current density at the peak (j_p) and in the passive range both increase with the OH$^-$ content, and passivation is observed at all concentrations. The peak current densities observed, correspond to etch rates ranging from 105 up to 523 nm min^{-1} for a concentration span of 0.1–1.0 M of KOH solution.

It is interesting to note that the current density required to passivate SiC is about two orders of magnitude larger than that needed for Si [18–20]. This difference is attributed to the presence of C in the SiC lattice [13]. Furthermore, for silicon
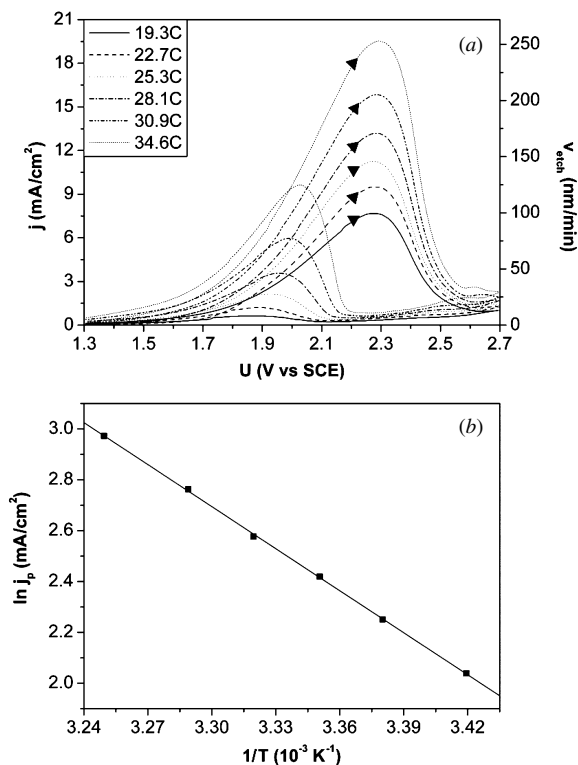
Figure 2. Influence of temperature on the j–U characteristics for p-type 4H-SiC in 0.1M KOH solution (*a*) and an Arrhenius plot showing the logarithm of the peak current density as a function of the reciprocal temperature (*b*).

Figure 3. Current density-potential plots at different light intensities for n-type 6H-SiC in 0.1M KOH solution at 22.5 °C. A focussed light source was used.

Figure 4. The dependence of the photocurrent at 0.625 V on the illumination intensity at different KOH concentrations in 0.5M K_2SO_4 for n-type 6H-SiC at 23 °C. The light source was not focussed.

a much larger hysteresis is observed which could be related to a difference in oxide morphology; even in 5M KOH at 60 °C it takes about 3 min for the passivating oxide to be removed.

The influence of temperature on the current–potential characteristics is shown in figure 2(*a*). The experiments were performed in 0.1M KOH solution. The peak current density depends strongly on temperature; it increases exponentially with increasing temperature. The etch rate, depicted on the right axis of figure 2(*a*), increases by a factor of 2.55 on a 15.3 °C temperature increase.

Figure 2(*b*) shows an Arrhenius plot of the logarithm of j_p versus reciprocal temperature. A straight line is obtained. From the slope an activation energy of 45.8 kJ mol^{-1} was calculated, which is typical for kinetically controlled reactions [21].

3.2. Photoelectrochemistry of n-type SiC

Figure 3 shows current density–potential plots measured at different light intensities for an n-type 6H-SiC electrode. The plots were recorded in 0.1M KOH solution at 22.5 °C and a focussed light source was used. In the onset of the photocurrent, electron–hole recombination competes with the anodic dissolution reaction. Since surface defects act as recombination centres, defect areas etch more slowly and are therefore revealed as hillocks (see the following section). At 'low' light intensity (0–28%), the photon flux is smaller than the flux of OH$^-$ ions from solution to the surface; the photocurrent reaches a constant value at positive potentials and this limiting photocurrent is directly proportional to the light intensity (figure 3). At high light intensity (100%),
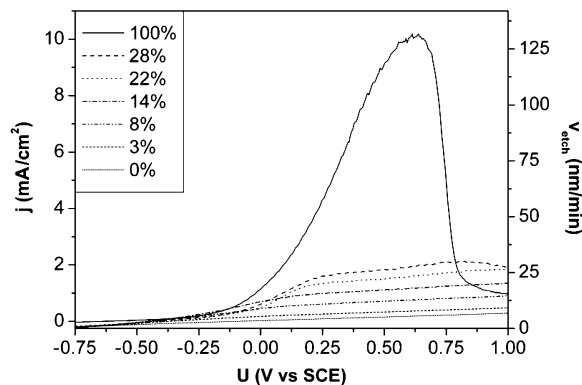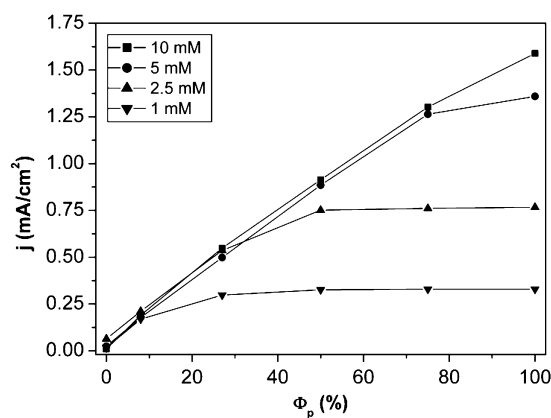
the electrode passivates due to the formation of a sparingly soluble oxide, as in the case of p-type SiC (figure 1). The j–U characteristics of 4H-SiC are similar, although the peak potential is 360 mV more negative than that of 6H (see section 3.4). At potentials in the vicinity of the peak, characteristic current oscillations are observed, due to the formation and dissolution of the passivating oxide [13]. At higher light intensities, not shown here, etch rates of 350 nm min^{-1} can be obtained in the pre-peak range (at 0.3 V). The root-mean-square roughness of the surface, evaluated within an area of 25 μm^2, is about 20 nm.

Two regimes are clear from the results of figure 3: at low photon flux, the limiting photocurrent is directly dependent on light intensity; at the highest photon flux, complete passivation occurs. Results shown in figure 4 indicate that the transition between these two regimes may be tuned by the experimental conditions. The limiting photocurrent was measured as a function of the photon flux for various OH$^-$ concentrations in the low concentration range ($\leqslant$10 mM) at 23 °C. An unfocussed light source was used. From figure 4 it is clear that, for a given OH$^-$ concentration, the photocurrent increases with increasing light intensity and then levels off. This constant photocurrent at higher photon flux depends on OH$^-$ and increases with increasing electrode rotation rate and concentration; this shows that in this intensity range, OH$^-$
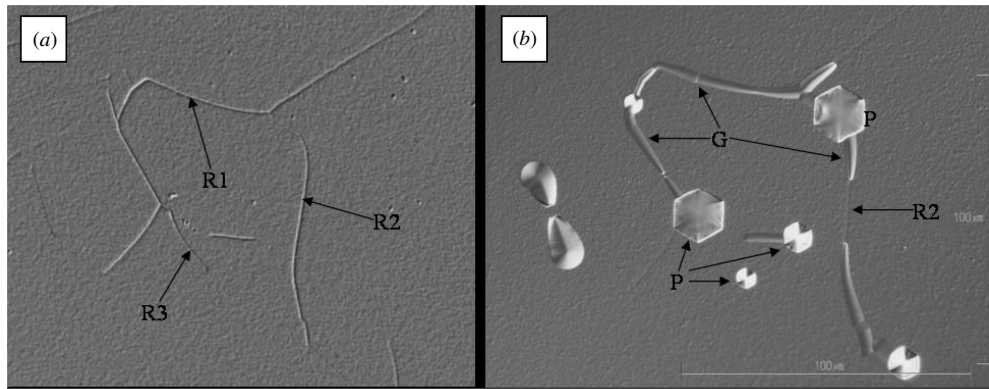
Figure 5. DIC images of a 4H-SiC substrate after open-circuit photoetching in 0.02M KOH solution for 30 min (*a*) and subsequent etching in molten E+M at 520 °C for 5 min (*b*).
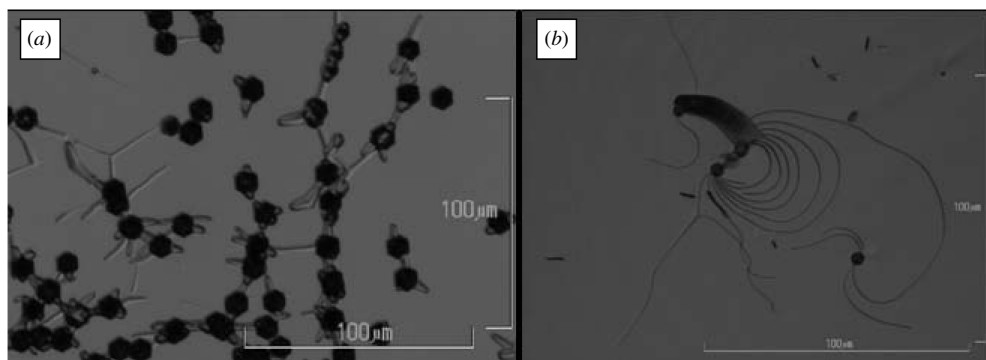

Figure 6. DIC image of a 4H-SiC substrate after etching in molten E+M at 520 °C for 5 min (*a*), DIC image of dislocations parallel to the surface revealed by open-circuit photoetching of a SiC substrate (*b*).

ion transport to the surface is rate limiting. These are the conditions required for electropolishing. Similar results have been observed previously with GaAs [21] and GaN [17]. For the 10 mM solution the dissolution rate is 20 nm min^{-1}; this can, in principle, be increased.

3.3. Applications of anodic etching: defect revealing

Open-circuit photoetching was used to reveal crystallographic defects in n-type SiC. Etching under these conditions corresponds to anodic etching at low current densities (see section 2).

Open-circuit photoetching of SiC reveals dislocations parallel to the surface in the form of ridges, as is clearly seen in figure 5(*a*). The dislocations form a kind of 3D network in this sample. Subsequent etching in a molten E+M etch shows the presence of a few dislocations perpendicular to the surface, the centre-symmetrical etch pits P in figure 5(*b*). These dislocations belong to this network but are not visible after photoetching. In addition, some ridges are transformed into grooves, some remain visible as ridges and some vanish (denoted by G, R2 and R3, respectively, in figure 5). The grooves G were formed on the dislocations present after photoetching inside the ridges under the surface, while the groove R2 represents a segment of a dislocation still remaining just under the surface after the second stage of etching. The vague ridge R3 was formed during photoetching on the residual strain field and/or impurity atmosphere of a dislocation,

which was just above the surface and therefore disappeared completely after etching in molten E+M (figure 5(*b*)).

The analysis of the images obtained after this two-stage etching procedure allows us to understand the peculiar etch features formed during E+M etching of some SiC substrates (as shown in figure 6(*a*)). Apart from the typical dislocation-related etch pits, numerous comet-like grooves were formed, which evidently represent segments of dislocations inclined with respect to the surface under small angles. Similarly, the ridges due to photoetching in figure 6(*b*) are formed on dislocations parallel to the surface and pinned by a cluster of macro-pipes.

Defect-selective etching using molten salts was performed mainly on the Si-polar face of SiC substrates. Simultaneous etching of wafers polished on both sides shows that dislocations are revealed on both the Si- and the C-face. In figure 7, the pits formed on the same low angle dislocation boundary are shown. The pits on the C-face are smaller than those on the Si-face, most probably due to the fact that the dislocation-free matrix on the C-face is dissolved during etching while the Si-polar matrix remains intact.

3.4. Applications of anodic etching: layer-selective etching

On the basis of these electrochemical results and our experience with other semiconductors [21], we can speculate on possible material-selective etching applications. Figure 8(*a*) shows *j*–*U* characteristics for n-type and p-type 4H-SiC and n-type 6H-SiC. The experiments were performed
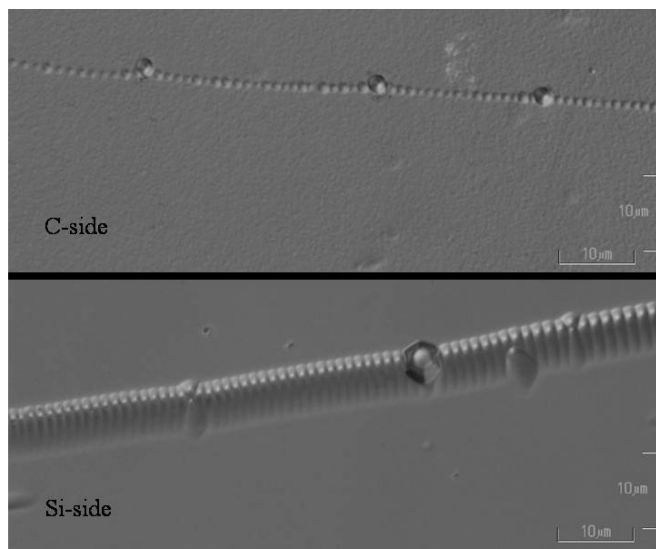
Figure 7. DIC images of a double-sided polished SiC wafer after simultaneous etching in a molten eutectic of NaOH/KOH at 500 °C for 5 min.
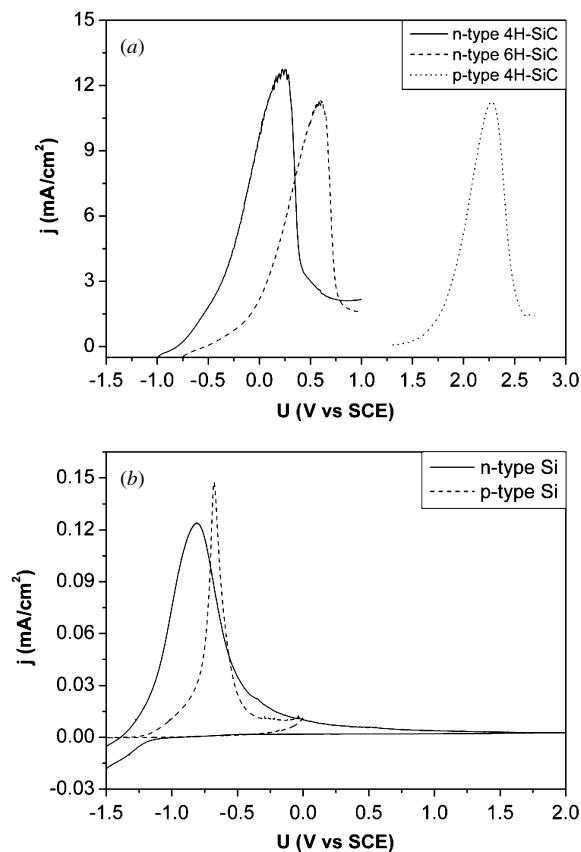

Figure 8. Current density–potential plots recorded for n-type and p-type SiC (*a*) and Si (*b*) in 0.1M KOH solution at 22.5 °C.

in 0.1M KOH solution at 22.5 °C. The n-type electrodes were illuminated at high light intensity (focussed light source, 100%). As can be clearly seen, n-type SiC dissolves at a much more negative potential than p-type SiC. These characteristics show that, under illumination, n-type material can be selectively removed because p-type SiC does not dissolve in this potential range. Selective etching of p-type with respect to n-type is also possible, as n-type SiC does not

etch in the dark. These features could, for example, be utilized for revealing the position of a p/n junction in devices or the selective etching of such junctions.

Since in MEMS applications, SiC is generally grown on Si [5–7], material-selective etching of such systems may be interesting. For comparison, the *j–U* characteristics of Si in 0.1 M KOH solution at 22.5 °C are shown in figure 8(*b*). In contrast to SiC, Si (both p-type and n-type) etches chemically in alkaline solution, i.e. at open-circuit potential. This means that selective etching of Si with respect to SiC is simple. Like SiC, Si is passivated at potentials positive with respect to its open-circuit value (see figure 8(*b*)). In the passive range, chemical etching of Si is prevented by the protecting oxide on the surface; this forms the basis for an important etch-stop mechanism in Si MEMS [22, 23]. Unlike n-type SiC, n-type Si does not require illumination to give anodic current; intermediates of the chemical etching reaction generate current by electron injection into the conduction band of the semiconductor [18, 19, 24, 25]. An important difference between the two semiconductors is that Si passivates anodically at considerably more negative potentials than SiC (compare figures 8(*a*) and (*b*)). This property can be exploited for the selective etching of p-type SiC (in the dark) or n-type SiC (under illumination); in both cases the potential is maintained at a value in the passive range of Si.

The large activation energy for anodic etching of p-type SiC indicates that dissolution of the solid is surface, i.e. kinetically, controlled. This suggests that anisotropic etching of the semiconductor should be possible.

4. Conclusion

High anodic etch rates can be obtained for both p-type SiC in the dark and n-type under illumination. The dissolution rate of SiC strongly depends on KOH concentration and temperature. At high anodic potential, surface passivation is observed. It was found that the dissolution of SiC in KOH solution is under kinetic control. It is shown that open-circuit photoetching of n-type SiC in KOH solution is a strong tool for revealing defects. Furthermore, the electrochemical properties of p-type and n-type SiC and Si in KOH solution should, in principle, allow for layer-selective etching.

Acknowledgments

References

[1] Katsuno M, Ohtani N, Takahashi J, Yashiro H and Kanaya M 1999 *Japan. J. Appl. Phys.* **38** 4661
[2] Di Ventra M and Pantelides S T 2000 *Phys. Rev. Lett.* **85** 1782
[3] Wang S W, Di Ventra M, Kim S G and Pantelides S T 2001 *Phys. Rev. Lett.* **86** 5946
[4] Willander M, Friesel M, Wahab Q U and Straumal B 2006 *J. Mater. Sci.-Mater. Electron.* **17** 1

[5] Connolly E J, Timmer B, Pham H T M, Groeneweg J, Sarro P M, Olthuis W and French P J 2005 *Sensors Actuators* B **109** 44

[6] Sarro P M 2000 *Sensors Actuators* A **82** 210

[7] Cong P and Young D J 2005 *J. Micromech. Microeng.* **15** 2243

[8] Okojie R S, Ned A A and Kurtz A D 1998 *Sensors Actuators* A **66** 200

[9] Okojie R S, Ned A A, Kurtz A D and Carr W N 1998 *IEEE Trans. Electron Devices* **45** 785

[10] Yih P H, Saxena V and Steckl A J 1997 *Phys. Status Solidi* b **202** 605

[11] Weyher J L, Lazar S, Borysiuk J and Pernot J 2005 *Phys. Status Solidi* **202** 578

[12] van de Lagemaat J, Vanmaekelbergh D and Kelly J J 1998 *J. Appl. Phys.* **83** 6089

[13] Dorp D H v and Kelly J J 2007 *J. Electroanal. Chem.* **599** 260

[14] Kato M, Ichimura M, Arai E and Ramasamy P 2003 *Japan. J. Appl. Phys.* **42** 4233

[15] Shor J S and Kurtz A D 1994 *J. Electrochem. Soc.* **141** 778

[16] Shor J S, Grimberg I, Weiss B Z and Kurtz A D 1993 *Appl. Phys. Lett.* **62** 2836

[17] Macht L, Kelly J J, Weyher J L, Grzegorczyk A and Larsen P K 2005 *J. Cryst. Growth* **273** 347

[18] Xia X H and Kelly J J 2001 *Phys. Chem. Chem. Phys.* **3** 5304

[19] Xia X H, Ashruf C M A, French P J, Rappich J and Kelly J J 2001 *J. Phys. Chem.* B **105** 5722

[20] Philipsen H G G and Kelly J J 2005 *J. Phys. Chem.* B **109** 17245

[21] Notten P H L, van den Meerakker J E A M and Kelly J J 1991 *Etching of III–V Semiconductors* (Oxford: Elsevier Advanced Technology)

[22] Connolly E J, French P J, Xia X H and Kelly J J 2004 *J. Micromech. Microeng.* **14** 1215

[23] Collins S D 1997 *J. Electrochem. Soc.* **144** 2242

[24] Allongue P, Costakieling V and Gerischer H 1993 *J. Electrochem. Soc.* **140** 1018

[25] Raisch P, Haiss W, Nichols R J and Schiffrin D J 2001 *J. Phys. Chem.* B **105** 12508